BULLETIN OF THE IRAQ NATURAL HISTORY MUSEUM
Iraq Natural History Research Center & Museum, University of Baghdad
https://jnhm.uobaghdad.edu.iq/index.php/BINHM/Home
Copyright © Bulletin of the Iraq Natural History Museum
Online ISSN: 2311-9799, Print ISSN: 1017-8678

Bull. Iraq nat. Hist. Mus.
(2025) 18 (3): 739-763. https://doi.org/10.26842/binhm.7.2025.18.3.0739

ORIGINAL ARTICLE

CLASSIFYING FLUVIAL LANDFORMS USING GEOSPATIAL MODELING IN AL-ASHAALI WATERSHED, IRAQI SOUTHERN DESERT

Bashar F. Maaroof *♦, Hashim H. Kareem **, Jaffar H. Al-Zubaydi ***, Rayan G. Thannoun ****, Manal Sh. Al-Kubaisi *****, Ban AL- Hasani ******, Mawada Abdellatif ****** and Iacopo Carnacina ******

*Babylon Center for Civilization and Historical Studies, University of Babylon, Hillah, Babil, Iraq.
**Department of General Sciences, College of Basic Education, University of Misan, Misan, Iraq.
***Department of Applied Geology, College of Science, University of Babylon, Babil, Iraq.
****Remote Sensing Center, University of Mosul, Mosul, Iraq.
*****Department of Geology, College of Science, University of Baghdad, Baghdad, Iraq.
****** Civil Engineering and Built Environment Department, Faculty of Engineering Technology, Liverpool John Moores University, Liverpool L3 5UX, UK.
♦Corresponding author: basharma@uobabylon.edu.iq

Received: 13 Feb. 2025, Revised: 27 May 2025, Accepted: 29 May 2025, Published:20 June 2025

This work is licensed under a Creative Commons Attribution 4.0 International License

ABSTRACT

This study examines the Al-Ashaali drainage basin, a watershed in the southern Iraqi desert, which constitutes a hydro-geomorphological system within the lower valleys region according to Iraq's geomorphological classification. The study uses a digital elevation model to classify the landforms of the watershed. Landform maps from the Shuttle Radar Topography Mission (SRTM) were combined with topographic maps to understand the formation of landforms. Geospatial simulation models were developed to create a simplified geomorphological base map. The data was analyzed utilizing ArcGIS software, which included color mapping tools, topographic maps, as well as geological and hydrological maps. The study aims to enhance the interpretation and geomorphological analysis of the watershed's landform characteristics. The Dutch Geosciences Institute (ITC) geomorphological classification system was used to categorize the landforms. The results indicated that the valleys in the study area are significant terrain due to their desiccation during the Quaternary period and their current location in arid regions. They exhibit fluvial erosion and are associated with Al-Ashaali watershed and Abu Hadair watershed in its western and southwestern areas. Rijlat Al-Tuwaitha is characterised by "captivity elbow" and "wind gaps", due to the accelerated flow of one river. The erosion plain is affected by erosion factors, including river sedimentation, floodplains, river islands, and braided streams. Alluvial fans develop in regions with steep slopes and lowlands, while floodplains are created by sediments carried by valleys and streams from steep highlands.

Braided streams undergo multiple cycles of deposition and erosion, and most flora in the region consists of pioneer species.

Keywords: Al-Ashaali, Landforms, SRTM, Topography, Watershed.

INTRODUCTION

Landform classification is essential for comprehending terrain surface characteristics and landform development. In In earlier decades, the primary objectives were to categorise the land surface according to various methods developed through discrete or complex geomorphic classifications (Ghosh and Bera, 2023). During that period, most geomorphologists believed that the primary objective of geomorphological mapping was to highlight the processes that predominantly influence and leave their unique marks on landforms (Rong *et al*., 2022). Since 2000, the objectives of the geomorphic mapping methodology have undergone significant transformation, directly influencing the processes for selecting suitable land use planning and enhancing sustainable agricultural practices (Martins *et al*., 2016). The methodological perspective has undergone rapid transformation due to technological advancements, as previous techniques were both time-consuming and costly (Lin *et al*., 2022). Scientists recognize contemporary geomorphological mapping and landform classification methods for emphasizing theme-based scientific classification instead of comprehensive scientific mapping (Ghosh and Bera, 2023).

Conventional landform classification and mapping primarily relied on field investigations to manually interpret topographic maps and aerial photographs, relying significantly on qualitative and subjective expert judgment (Amine *et al*., 2019). Moreover, field investigations and manual recognition inherently entail burdensome tasks that are both time-consuming and labour-intensive (Pereira *et al*., 2013). Recently, scientists have employed geospatial techniques to gather data on landform structures and configurations, judgment by high-precision digitised mapping (Mokarrama and Hojati, 2018). Due to the acquisition of diverse data sources like the digital elevation models (DEM), various automated methods- mainly digital landform classification techniques- have gradually replaced traditional methods in recent years (Zhou *et al*., 2023). The advancement of DEM data acquisition has established landform classification via DEM as a primary technique and focal point in the field, due to its high accuracy and logical classification framework (Burnelli *et al*., 2023). However, descriptions of fluvial landforms remain consistent, hindering our ability to compare the patterns of these features across river systems, even when employing analogous nomenclature. River landforms have been referred to as channel geomorphic units, habitat units, morphological units, and morphogenetic units; for simplicity, we refer to these features as geomorphic units (Guitet *et al*., 2013).

Geomorphic maps help us understand and measure the connections between processes and the factors controlling them (Mokarram *et al*., 2015; Wheaton *et al*., 2015; Manosso *et al*., 2021; Al-Sababhah, 2023). They also help us examine river evolution and adaptive capacity, and illustrate geomorphic change over time. These maps typically condense spatially continuous data (e.g., topography) into a discrete representations of the essential characteristics defining the rivers landscape (Carrión-Mero *et al*., 2022). We assert that the fluvial geomorphic community lacks a universally applicable framework for consistently identifying river features, as geomorphic mapping and identifying river building blocks depend on classification (Zabaleta *et al*., 2020). This issue is equally important for both field mapping interpretation and analysing remotely sensed data. All maps are derived from foundational conceptual models and the accessible data used in their creation (Mohamed, 2020). When executed effectively, geomorphic maps offer insight into the characteristics, patterns, and arrangement of landforms. (Mokarram *et al*., 2015).

This study aims to determine the spatial distribution of different riverine landforms in Al-Ashaali catchment. The objectives are to: (a) provide a geomorphological map of the catchment at a scale of 1:50,000 (see main map), (b) establish a time frame to trace the evolution of landforms during the Pleistocene era, (c) identify the dominant processes controlling the geomorphological evolution, and (d) provide a detailed map of the Al-Ashaali catchment surface, and link the spatial distribution of landforms to the geological, climatic, and hydrological setting to so as identify their correlations and interpret the formation of landforms in the study area.

MATERIALS AND METHODS

Study area: Al-Ashaali Watershed is located in the eastern part of the southern Iraqi desert, within the administrative borders of Al-Muthanna Province (Al-Jiburi *et al*., 2015). It is bordered to the north, west, and southwest by Abu Hadair Watershed and to the east and southeast by Al-Kaseer Watershed (Map 1). Al-Ashaali Watershed is located between latitudes (30°26′27.343″N–30°56′56.184″N) north and longitudes (45°10′49.107″E–45°39′31.4″E) east. Al-Ashaali is one of the seasonal watersheds in the southern Iraqi desert, situated within the lower valley region. The watershed area is 1071.19 km^2, with a perimeter of 241.474 km, and a total length of 71.417 km. Its direction starts from its upper sources near Rijilat Abu Hadair and Barbak Al-Diyud and ends at its mouth near the Al-Sulaibate depression (Al-Abadi and Shahid, 2016). Al-Ashaali Watershed is characterised by a relatively low-altitude plateau and a gradual slope from the southwest to the northeast.

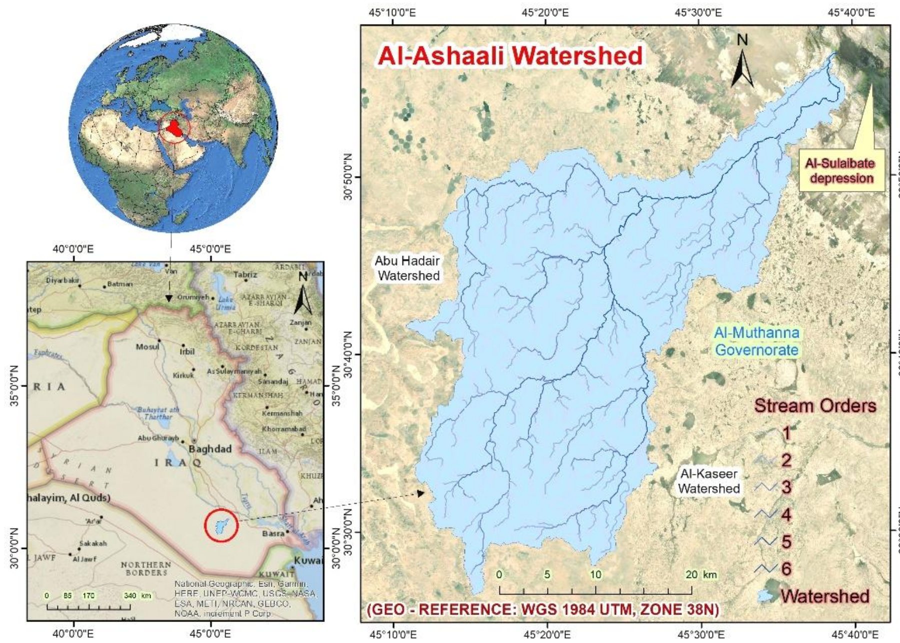

Map (1): Location of Al-Ashaali watershed in Iraq.

The average gradient is 2.33 m/km, and the watershed is distinguished by variations in elevation across its sections. The maximum elevation located at its upper sources in the southwestern region, attained 180 meters above mean sea level (AMSL) (Maps 2, 3; Diag. 1). The minimum elevation attained is 20 meters AMSL in the estuaries region adjacent to the Al-Sulaibate depression (Maaroof, 2022a). Al-Ashaali exhibits heightened ruggedness in its upper regions, delineating the source area between the 180- and 120-meter AMSL contour lines (Al-Jiburi and Al-Basrawi, 2009). This region exemplifies the youth stage in the Davisian cycle of watershed development, characterised by various topographic features, including plateaus, hills, fault edges, and other landforms. The central region of Al-Ashaali, indicative of the maturity phase of the Davisian geomorphological cycle, lies between 120 and 70 meters AMSL. All landforms present in the southern Iraqi desert are depicted within it. It is less precipitous and rugged than the initial region. The level diminishes progressively until it attains the Estuary Region, indicative of the old-age phase of the geomorphological cycle, which is situated between contour lines of 70 to 20 meters AMSL (Ma'ala, 2009).

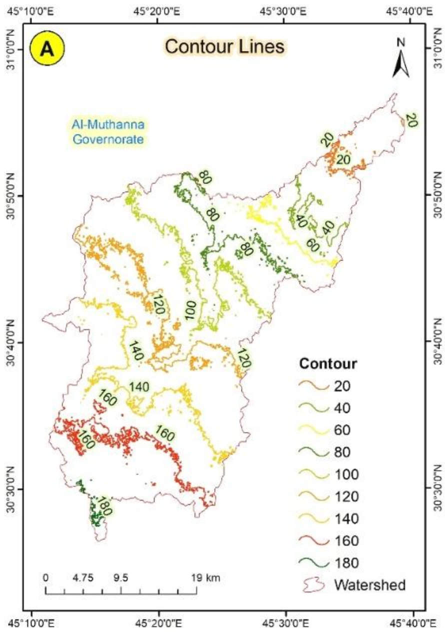

Map (2): (A) Contour lines, (B) Slope levels of Al-Ashaali watershed.

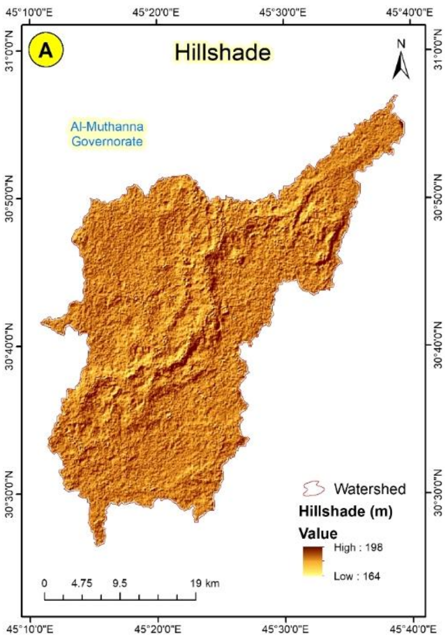

Map (3): The hillshade and geomorphological phases of the Al-Ashaali watershed.

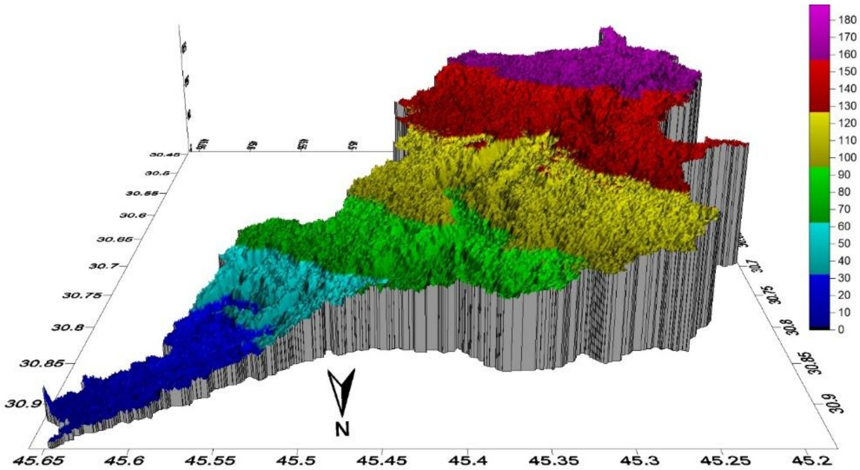

Diagram (1): The 3D model of the Al-Ashaali watershed.

The study area comprises geological formations that differ based on their sedimentary environments. Some formations were deposited under continental conditions due to marine regression, while others formed under marine conditions due to marine transgression (Al-Jiburi and Al-Basrawi, 2009). The exposed rock formations in the study area differ based on their depositional environments, with some having deposited under continental conditions due to marine regression (Map 4). Conversely, others were deposited under marine conditions due to marine advancement. The ages of these formations span from the Upper Eocene Epoch of the Tertiary period to the Holocene Epoch of the Quaternary period (Sissakian *et al*., 2013). The instances of marine subsidence and submersion result from land movements experienced by the region throughout its geological history, leading to alterations in sea level and climatic conditions. The study area features multiple geological formations, notably the Dammam formation, which is visible in the basin's northern section and overlain by a variable thickness of sand plate deposits (Ali *et al*., 2021). The Al-Ghar Formation, located in the central and western regions of the basin, is partially obscured by aerobic sediments. The Al-Zahra formation is situated in the southern areas, comprising sandy mudstone and sandstone limestone. (Al-Jiburi and Al-Basrawi, 2015).

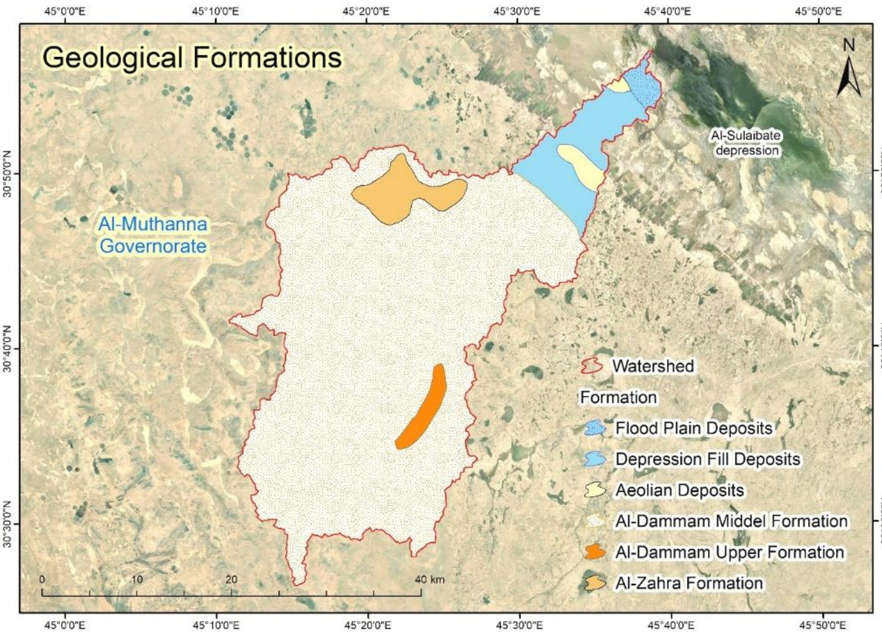

Map (4): Geological formations of the Al-Ashaali watershed.

Al-Ashaali watershed is categorised as having an arid climate (Maaroof *et al*., 2023). The data in Diagram (2) demonstrate that temperatures commence an ascent in March, attaining 18.2 °C, peaking in July at 36.2 °C, and than decreasing slightly in August to reach 35.3 °C. Conversely, temperatures can drop to 11.3 °C during the cold season, which lasts from late November to mid-April, differentiating Iraq from a tropical climate according to the Koppen classification (Maaroof and Kareem, 2020). The study area is marked by seasonal precipitation, occurring at intervals as showers that can rapidly escalate into torrents. Precipitation occurs from October to May, with an annual total of 96.5 mm. Rainfall in the study area exhibits both yearly and monthly variability (Al-Hasani *et al*., 2024). The prevailing winds in the study area come from the north and northwest. They are indistinguishable from the winds traversing the central regions of Iraq, particularly those over the sedimentary plain, as the winds above dominate these areas as well. The gusts are closely linked to atmospheric pressure distributions beyond the region's boundaries (Al-Hasani, *et al*., 2024). The annual average wind speed in the study area is 2.983 m/s, with an increase during the summer months, reaching 3.9, 2.9, and 2.6 m/s in June, July, and August, respectively. The mean wind velocity diminishes during winter (November, December, and January) to attain 2.4, 2.3, and 2.3 m/s, respectively (Maaroof *et al*., 2021).

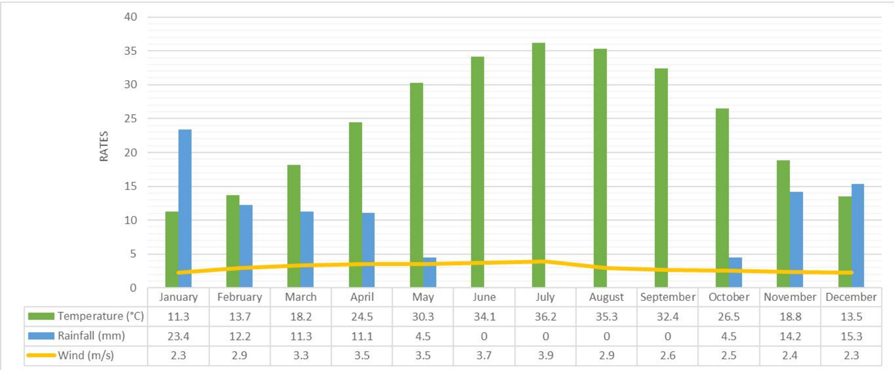

Diagram (2): Climatic data, including temperature, precipitation, and wind speed, for the study area from 1990 to 2020, sourced from the Al-Samawah Climatic Station. [From: Iraq | World Meteorological Organization (wmo. int)]

Al-Ashaali watershed is segmented into several sub-watersheds, each exhibiting distinct standard characteristics, as detailed below:

1. Al-Ashaali sub-watershed (1) (ASW1): This sub-watershed is situated in the upper regions of the main watershed, encompassing an area of 670.013 km², a perimeter of 202.030 km, and a length of 53.696 km (Tab. 1, Maps 5, 6).
2. Al-Ashaali sub-watershed (2) (ASW2): This sub-watershed is situated in the southwestern region of the main watershed, encompassing an area of 273.914 km², a perimeter of 108.950 km, and a length of 34.036 km.
3. Al-Ashaali sub-watershed (3) (ASW3): This sub-watershed is situated in the southeastern region of the primary watershed, encompassing an area of 184.918 km², a perimeter of 95.733 km, and a length of 28.719 km.

Table (1): The area, perimeter, and length of the Al-Ashaali sub-watersheds.

Sub-watersheds	Area (km^2)	Perimeter (km)	Length (km)
Al-Ashaali sub-watershed (1) (ASW1)	670.013	202.030	53.696
Al-Ashaali sub-watershed (2) (ASW2)	273.914	108.950	34.036
Al-Ashaali sub-watershed (3) (ASW3)	184.918	95.733	28.719

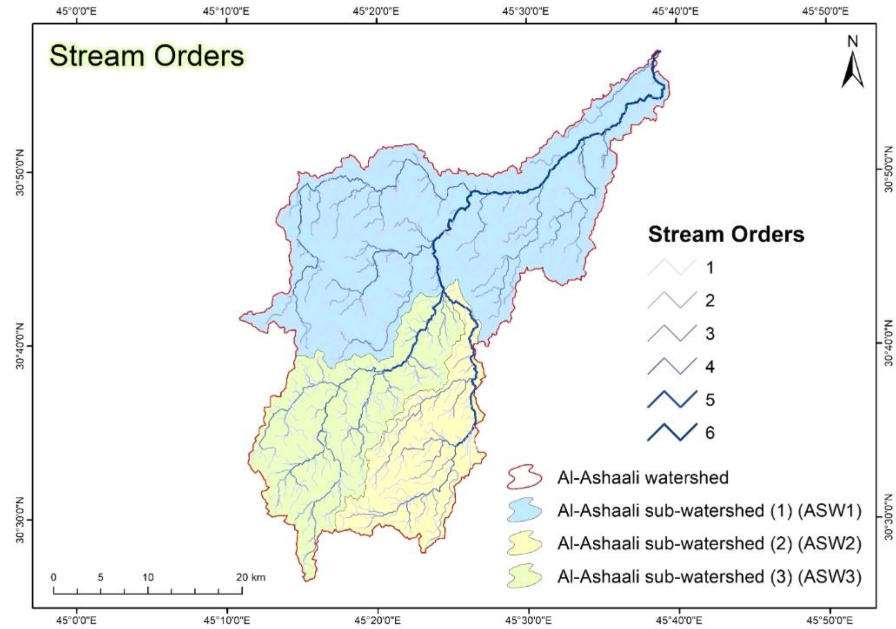

Map (5): Al-Ashaali stream orders and sub-watersheds.

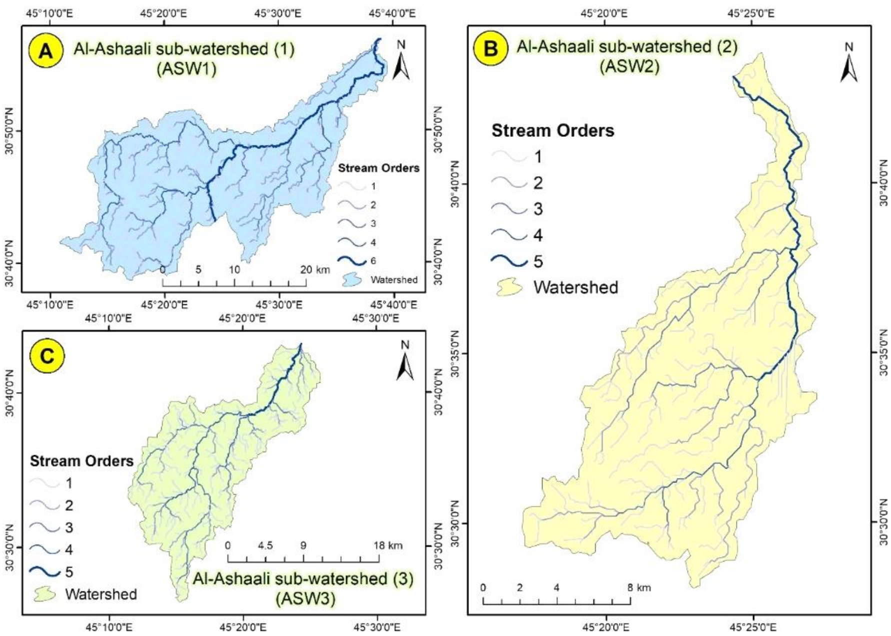

Map (6): Stream orders of Al-Ashaali sub-watersheds.

Data Collection: This paper examines the classification of landforms within Al-Ashaali catchment through digital elevation model (DEM) analysis. Choosing a high-resolution DEM as input data is imperative to classifying landforms (Martins *et al*., 2016). The dimensions and expanse of landforms exhibit aggregation relative to the spatial resolution characteristic (Map 7). Digital Elevation Models (DEMs) have consistently been utilised to ascertain the spatial resolution of satellite imagery. The landform maps produced by the baseline DEM from the Shuttle Radar Topography Mission (SRTM) were juxtaposed with topographic maps. The terrain data were analysed alongside geological and hydrological data to elucidate the formation of landforms in the study area. Geospatial simulation models of the terrain were developed to construct a simplified geomorphological base map encompassing the entire study area and to elucidate the relationships among various features. Each dataset was individually processed before being amalgamated as a sub-layer on the foundational terrain. The spatial correlation among multiple features and terrain characteristics was emphasised. The analysis and interpretation of the data primarily relied on direct visualisation and specific statistical characteristics of the features, including area/extent and thickness. The amalgamation of the various datasets was executed using ArcGIS software. ArcGIS software encompasses a diverse array of map design components. Various color tools and effects, such as transparency, lighting, and shading, were used to create legible maps that effectively conveyed the research content (Al-Sababhah, 2023; Yang *et al*., 2023).

Furthermore, 1:100,000 topographic maps from the General Authority of Survey of Iraq and 1:250,000 geological and hydrological maps from the Iraqi Geological Authority were utilised in Geosurviraqi. Upon inputting the data into the GIS via ArcGIS V.10.8, they were incorporated into a topological model as point layers. Alongside the extraction of the river drainage network at all levels, the principal watersheds and sub-watersheds were delineated and extracted as vector layers. Supplementary software applications utilized for spatial analysis included Google Earth Pro V.7.1, Arc GIS Earth V.2, Surfer V.10, and Global Mapper V.11. Following the creation of an integrated geospatial database for the study area, the interpretation stage and geomorphological analysis of the watershed's landform characteristics were enhanced using a set of geomorphological criteria. The geomorphological factors, processes, and stages were interconnected, and the development of the watershed's landform characteristics was assessed within the context of geomorphological analysis. The cartographic methods highlighted the spatial dimensions of the watershed's geomorphological features (Teofilo *et al*., 2019).

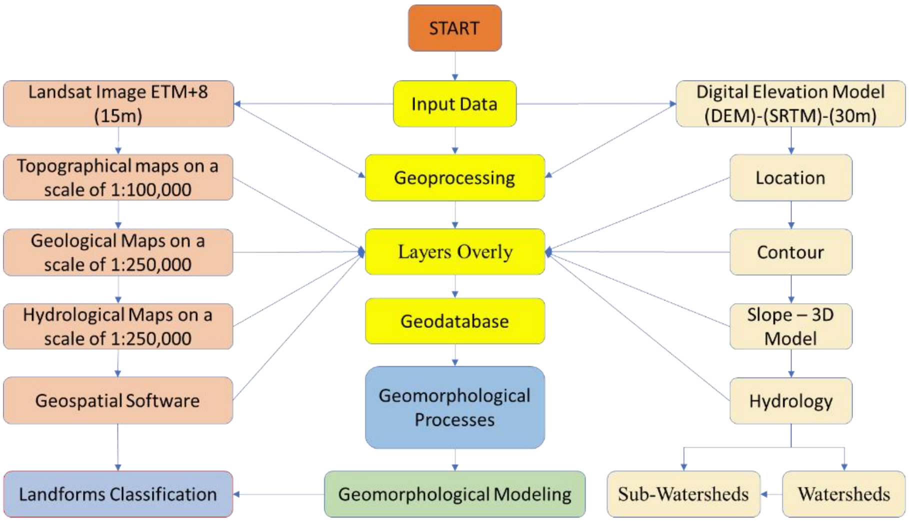

Diagram (3): Flowchart of methodology.

RESULTS AND DISCUSSION

Erosional fluvial landforms

Valleys: Valleys constitute a significant terrain in the study area, as flowing water excavated many of them under specific water drainage conditions during the Quaternary period (Maaroof, 2022b). These valleys (Map 8 – a) have been desiccated due to climatic alterations and their current location within an arid region. These valleys exhibit numerous features indicative of fluvial erosion. Nevertheless, they are situated in one of the most arid regions, with the sole water source currently being rainfall during brief intervals in winter and early spring. Many of these valleys traverse zones of weakness in the limestone formations, facilitating the activation of subsurface karst processes. These valleys experience ephemeral water flow following precipitation due to the elevated permeability of the rocks. As water traverses these valleys, it erodes fragile rocks, creating deep depressions (Maaroof, 2024).

Escarpments: This type of landform is associated with the central valleys along the river's banks or edges. Different geomorphological processes produce large amounts of broken rock debris below these edges, which are easily swept away by water erosion processes that transport rock fragments from one place to another (Kothyari *et al*., 2021). However, if water cannot transport these fragments, they accumulate at the base of the edges, forming a "galasiplane" (Morino *et al*., 2022). The analysis of satellite images indicates that these fragments- composed of solid limestone rocks resistant to geomorphological processes- accumulate below the edges of river channel banks, with heights ranging from 2 to 5 meters.

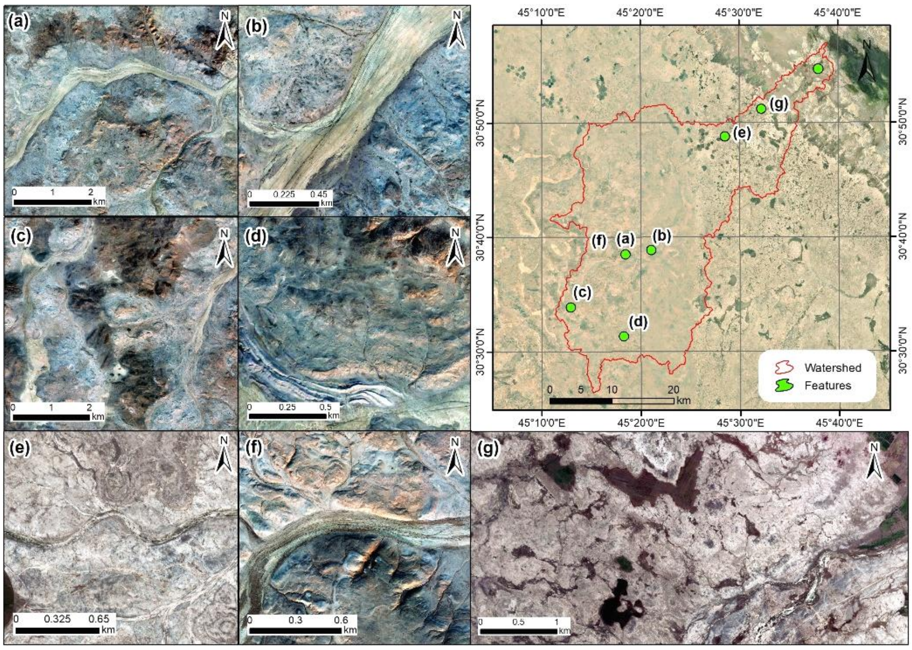

Map (8): Erosional fluvial landforms in Al-Ashaali watershed; (A) Valleys, (B) Escarpments, (C) Stream capture, (D) Badlands, (E) Meanders, (F) Cliffs, (G) Pediplain.

Stream capture: River captivity is a prevalent occurrence in the watersheds of the southern Iraqi desert. The geomorphological history of Al-Ashaali watershed reveals this phenomenon in conjunction with adjacent watersheds, particularly Abu Hadair watershed in its western and southwestern regions. Evidence exists that this occurs, particularly in the region known as Rijlat Al-Tuwaitha, where the sources of this basin converge with its two tributaries (Al-Saka'a and Abu Khasoufah) and the auxiliary Abu Hadair watershed. Features such as "Captivity elbow" and "wind gaps" have been observed. A "Captivity elbow" refers to the curved intersection between the captive river and the captured river, whereas "wind gaps" result from the contraction of the captured channel, forming a dry channel (Wheaton *et al*., 2015).

In the study area, river captivity occurs due to multiple factors, including the presence of a river with a steeper gradient than others, resulting in an accelerated flow that enhances the deepening of its valley. Furthermore, the rocks over which a river traverses exhibit low resistance to erosion, either due to their softness or the presence of structural weaknesses such as cracks, joints, and fractures. Consequently, this accelerates the river's vertical erosion process, hastening its retrogression and enabling it to appropriate the sources of another river. River captivity may arise from the expansion and alteration of river bends, resulting in the confluence of one river with the course of another.

Badlands: This landform is a consequence of a specific type of erosion induced by precipitation and water in arid and semi-arid areas. Infrequent but intense rainfall can generate torrents when the terrain is composed of cohesive clay, chalk, or gypsum sediments. The torrents rapidly erode the rocks, transforming the terrain into a complex network of grooves, gorges, and small pools interspersed with cliffs, rendering the area difficult to traverse (Mandal and Chakrabarty, 2021). This landform is prevalent in the central and southern regions of the study area, with elevations ranging between 2 and 3 meters, and is encircled by debris resulting from the weathering and erosion processes to which this area has been subjected. Alongside the sequence of brittle and rugged rocks, exposed rocks exhibit reduced complexity, facilitating their weathering and erosion. The absence of vegetation cover has facilitated the exposure of these areas' surfaces to weathering and erosion, as natural vegetation helps mitigate water erosion during rainfall in the study area.

Meanders: River courses exhibit curvatures due to the characteristics of the stage the river is traversing through. The curvatures are typically minimal in youth and early mature stages, becoming most pronounced in old age (Nagata *et al*., 2014). The river forms a meander in the study area through lateral erosion driven by geomorphological processes; the erosion resistance of the banks differs (Njenga *et al*., 2012). The development of the meander in the study area is chiefly attributable to a bank comprising a substantial proportion of sand and silt alongside a minor proportion of clay. This bank is highly susceptible to the lateral erosion processes that gradually degrade it. This phenomenon creates the external arch or concavity, characterised by a narrow bank with a steep gradient and significant depth. Geomorphological processes at concavities are destructive, whereas on the opposite banks of the meander, where water current velocity diminishes, sediments are deposited, forming a convex bank known as the internal arch (Maaroof and Kareem, 2022).

Cliffs: Rock cliffs are uniform, steep formations that rise vertically and semi-obliquely, exhibiting a gradient exceeding 40 degrees relative to the horizontal plane of the Earth's surface; when the slope attains 90 degrees, it is called a rock wall (Flor-Blanco *et al*., 2022). Their formation and development are linked to the system of horizontal stratification, the rock composition varying from hard to brittle layers of differing thicknesses, and the impacts of water erosion in all directions (Swirad and Young, 2022). The study area contains numerous geological features, including rock cliffs. These phenomena are particularly prevalent in areas where rivers meander and the cliff edges are eroded by retrogressive erosion, rockfall, and landslides along the cliffs and the flanks of the primary river valleys.

Pediplain: These are plains formed at the end of the Devonian erosion cycle, and the most important feature is their surface's flatness and lack of ruggedness. Their slope is simple, so it is almost insufficient to sustain river channels flowing slowly toward their estuaries (de Amorim *et al*., 2021). The erosion plain is not considered the final picture of how the earth's surface looks after a complete erosion cycle is over. It is always affected by different erosion factors that shape its overall geomorphological appearance. Large-scale erosion plains typically split into scattered remnants of a limited area, separated by various river channels (Mirzadeh *et al*., 2023). The remnants of the erosion plain vary in height depending on the size of the watershed and the river channel's level, which is higher in the source area than at the estuary (Mokarram *et al*., 2015).

The northern parts of the basin distribute the erosional plains. These parts are characterised by their severe dissection due to water erosion. These areas are situated at elevations ranging between 20 and 100 meters AMSL. They are underlain by Limestone and sandstone rocks connect these areas, and are covered by loose sediments derived from these materials. Both physical and chemical weathering processes expose the surface sediments, leading to their fragmentation. Sometimes, their color may change due to the interactions between their mineral components and raindrops. These plains represent an advanced stage of river erosion. However, fault movements in the region cut it into several faults at the start of their formation. In a later stage, the valleys would developed their drainage networks and gradually leveled the area, resulting in the formation of the erosional plain.

Depositional fluvial landforms

Valleys Deposits: River load is deposited when conditions are favorable- specifically when the river load surpasses its capacity, and the sediment volume exceeds the efficiency threshold of the river (Maaroof and Kareem, 2023). Sedimentation may transpire progressively along the river course, depending on the gradation of sediment size and the reduction in slope, water discharge, and flow velocity (Maaroof, 2025). The substantial materials that form a significant portion of the bed load, are deposited initially. In contrast, finer materials, including the suspended load, remain in movement and may eventually reach the river's estuary environment. The size of transported particles diminishes as we progress downstream from the basin's upper sources (Langbein and Schumm, 1958). Thornbury (1966) delineated the factors and conditions that contribute to sedimentation, characterised by a reduction in the river's capacity to transport sediments, resulting from a decrease in velocity as it transitions from higher to lower terrain, the formation of folds, or an increase in river meandering. Sedimentation occurs due to flood-induced river expansion and a decrease in water volume driven by climatic variations (Schumm, 1981).

Al-Ashaali watershed is distinguished by substantial sediment deposits that differ in quantity, size, and thickness across various sections of the basin. Rock masses, boulders, and unsorted sandy and calcareous clastic sediments characteriSes the upper strata's lower sections. In certain regions, the substrates consist of sediment-free rocks due to the steep gradient and surface runoff characteristics. The valley floors in the central areas of the basin are composed of sand, silt, and clay sediments, influenced by the valley's width, the volume of flowing water, and the types of rocks most susceptible to dissolution.

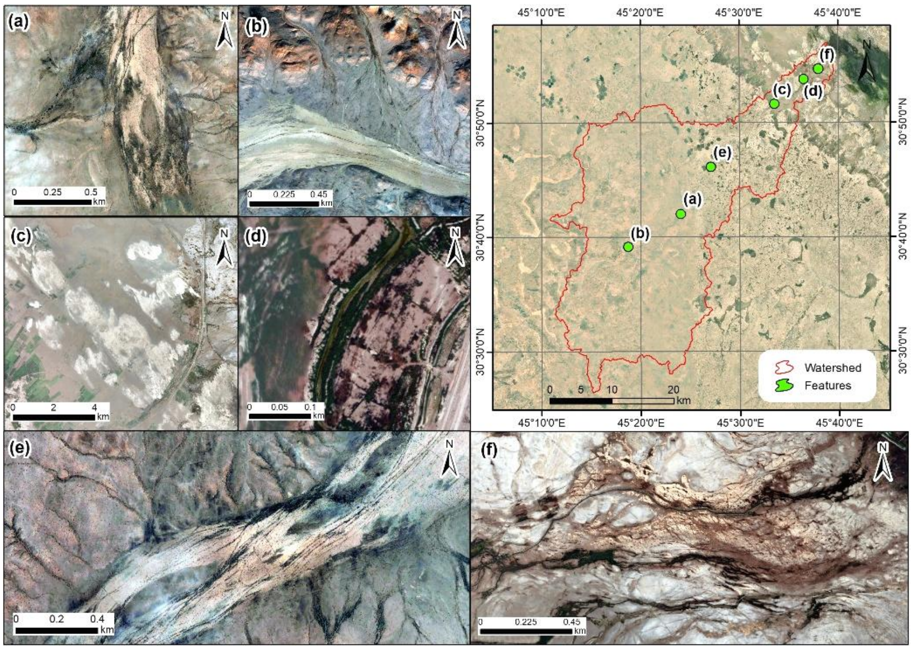

Map (9): Depositional fluvial landforms in Al-Ashaali watershed; [(A) Valleys Deposits, (B) Alluvial fans, (C) Flood plains, (D) Natural levees, (E) River islands, (F) Braided streams].

Alluvial Fans: They represent a type of river sedimentation in the study area, reflecting prior climatic conditions and geomorphological processes (Tebakari and Kita, 2015). This phenomenon is widely regarded as having formed due to the rainy climatic conditions of the Pleistocene and has experienced modifications, particularly during significant floods that periodically affect the watershed. Alluvial fans develop in regions where steep slopes- such as plateaus and elevated hills- converge with lowlands, including plains and valley bottoms, characterised by a dry or semi-arid climate (Hashemi *et al.*, 2018). The rivers within them are typically ephemeral, transporting substantial sediment while flowing rapidly over steep terrain shaped by diverse weathering processes. The flow velocity of these rivers abruptly diminishes as they approach neighboring lowlands, resulting in the deposition of much of their sediment load in the transitional zone in the transitional zone (Singh *et al.*, 2022). Coarse sediments are primarily deposited first, particularly in the central part of the river channel, where a barrier forms, causing the river to bifurcate into two additional branches. The bifurcation of rivers escalates, while the volume of water and sediment they transport diminishes as they progress away from the elevated area. Consequently, alluvial fans exhibit considerable thickness and coarse sediments in their upper sections adjacent to elevated areas. In contrast, their thickness diminishes, particle size reduces, and width expands as one move further from these highland regions (Chen and Capart, 2022).

Classifying fluvial landforms

Floodplains: Floodplains are located to the north of the study area, representing the lowest topographical feature. This plain was created by sediments carried by valleys and streams from steep highlands, which facilitated the acceleration of water currents and enhanced erosion in these regions. As the slope decreases, since valleys and streams cut through high areas with steep slopes and flow into flat areas, the speed of the water flow slows, causing the sediments it carries to settle. Floodplains develop due to recurrent surface runoff. The overall gradient of these plains is from southwest to northeast, consistent with the slope of the study area. Streams, waterways, and minor valleys occasionally punctuate these plains, and banks intermittently bisect them.

Natural Levees: Elevated hills delineate the floodplain from the riverbed. When silt accumulates on either side of a river, it creates dams and results in a gradual water flow (Wang *et al*., 2012). Occasionally, these dams fail under the pressure of floodwaters inundating the floodplain. The elevation of these dams in the rivers of the study area is 5 m above the floodplain level on either side of the river. Natural dams in the study area are frequently linked to meandering, whereas they have not been observed in braided rivers, which deposit gravel and coarse sand within their channels rather than on their banks (Lee *et al*., 2023).

River Islands: Water encircles these land areas, which are formed entirely due to sedimentation in the riverbed (Raslan and Salama, 2015). The formation of river islands is associated with the deposition of sedimentary materials such as clay, silt, sand, and gravel in stratified layers, beginning at the riverbed and progressing to the water's surface (Sadek, 2013). The study area correlates the formation of river islands with the augmentation of sediments transported by the river. The river's diminishing capacity to transport sediments forces it to deposit its load on the riverbed, obstructing the waterway. Over time, these barriers proliferate and enlarge due to ongoing sedimentation, ultimately transforming into islands within the river's course. Most river islands in the study area form at bends, where reduced water velocity facilitates sediment deposition and land formation.

Braided Streams: Braided streams are distinctive geomorphic formations characterised by wider riverbeds through which water flows in multiple channels amidst sediment. They are characteristic of the middle sections of rivers (Xia *et al*., 2025). The sediment deposition in a midchannel bar redirects water towards the banks, where it exerts increased force, resulting in bank erosion and stream widening. A sediment-laden stream may deposit numerous bars within its channel, widening a continuous stream as additional bars accumulate. A stream generally undergoes multiple cycles of deposition and erosion, mainly when its discharge varies (Olsen, 2021). The stream may accumulate sediment in its primary channel, transforming into a braided stream that flows through a network of interconnected rivulets surrounding multiple bars. A braided stream typically possesses a broad, shallow channel. The entire riverbed is generally submerged during floods, rendering smaller branches invisible (Coulthard, 2005). A stream typically becomes braided when it is significantly burdened with sediment, especially bed load, and has easily erodible banks. The braided pattern forms in deserts when a sediment-rich stream loses water via evaporation and percolation into the soil.

Braided streams are morphologically unstable habitats. The majority of the flora in these regions consists of pioneer species (Gran and Paola, 2001).

CONCLUSIONS

Valleys in the study area are significant terrain due to their desiccation during the Quaternary period and their current location within an arid region. These valleys exhibit numerous features indicative of fluvial erosion, and are located in some of the driest regions, where rainfall is the sole water source. River captivity occurs when one river expands its course at the detriment of another, resulting in profound depressions. This landform is associated with central valleys situated along rivers banks or edges. It is related to Al-Ashaali watershed and Abu Hadair watershed in its western and southwestern regions. Rijlat Al-Tuwaitha is a region where the sources of this basin converge with its two tributaries Al-Saka'a and Abu Khasoufah along with the auxiliary Abu Hadair watershed.

The geomorphological history of Al-Ashaali watershed reveals this phenomenon in conjunction with adjacent watersheds, particularly the Abu Hadair watershed in their western and southwestern regions. Rijlat Al-Tuwaitha is characterised by features such as "captivity elbow" and "wind gaps," which occur when one river exhibits a steeper gradient than others, resulting in an accelerated flow that enhances the deepening of its valley. The absence of vegetation cover facilitated the exposure of these areas' surfaces to weathering and erosion. The study area contains numerous geological features, including rock cliffs, which are particularly prevalent in areas where rivers meander and the cliff edges are eroded by retrogressive erosion, rock fall, and landslides along the cliffs and flanks of primary river valleys. The erosion plain is affected by different erosion factors that shape its overall geomorphological appearance. River sedimentation occurs when the river load exceeds its capacity and the sediment volume exceeds its efficiency threshold. This process can occur progressively along the river’s course, depending on sediment size gradation, slope reduction, water discharge, and flow velocity.

Al-Ashaali watershed is characterised by substantial sediment deposits in various basin sections, reflecting prior climatic conditions and geomorphological processes. Alluvial fans develop in regions where steep slopes converge with lowlands, transporting substantial sediment while flowing rapidly over steep terrain. Coarse sediments are primarily deposited first, particularly in the river channel's centre, where a barrier forms, causing the river to bifurcate into two additional branches. As the flows progress from the elevated area, their thickness diminishes, particle size reduces, and width expands. Floodplains are located in the north of the study area, representing the lowest topographical feature. These are formed by sediments carried by valleys and streams from steep highlands, facilitating water currents' acceleration and enhanced erosion. River islands form when sedimentation in the riverbed, and diminishing the river’s ability to transport sediments forces it to deposit its load on the riverbed, partially obstructing the water flow. Braided streams, another distinctive geomorphic feature, are characterized by wider riverbeds through which water flows in multiple channels amidst sediment. These streams undergo numerous cycles of deposition and erosion, mainly when their discharge levels vary. Braided pattern forms in deserts when a sediment-rich stream loses water through evaporation and percolation into the soil. The majority of the flora in that region consists of pioneer species.

ACKNOWLEDGEMENTS

The authors thank Babylon Center for Civilization and Historical Studies at the University of Babylon, Department of Geology at the University of Babylon, and Department of Civil Engineering and Built Environment at Liverpool John Moores University for the scientific support provided throughout the study.

CONFLICT OF INTEREST STATEMENT

"The authors declare no conflict of interest".

LITERATURE CITED

Al-Abadi, A. M. and Shahid, S. 2016. Spatial mapping of artesian zone at Iraqi southern desert using a GIS-based random forest machine learning model. *Modeling Earth Systems and Environment*, 2: 96. [CrossRef]

Al-Hasani, B., Abdellatif, M., Carnacina, I., Harris, C., Al-Quraishi, A. M. F. and Maaroof, B. F. 2024. Assessing climate change impacts on rainfall-runoff in Northern Iraq: a case study of Kirkuk Governorate, a Semi-Arid Region. *In*: A. Al-Quraishi, Negm, A. and Benzougagh, B. (Eds.), Climate Change and Environmental Degradation in the MENA Region. Springer Nature, p. 93-111. [CrossRef]

Al-Hasani, B., Abdellatif, M., Carnacina, I., Harris, C., Al-Quraishi, A., Maaroof, B. F. and Zubaidi, S. L. 2024. Integrated geospatial approach for adaptive rainwater harvesting site selection under the impact of climate change. *Stochastic Environmental Research and Risk Assessment*, 38(3): 1009-1033. [CrossRef]

Ali, A. H., Ali, K. K. and Al-Shamma'a, A. M. 2021. Surface basins evaluation of the southern desert, West Iraq. *Iraqi Journal of Science*, 62(7): 2272-2285. [CrossRef]

Al-Jiburi, H. K. and Al-Basrawi, N. H. 2009. Sratigraphy of Iraqi Southern Desert. *Iraqi Bulletin of Geology and Mining*, *Special Issue, 2009: Geology of Iraqi Southern Desert*: 77-91.

Al-Jiburi, H. K. and Al-Basrawi, N. H. 2015. Hydrogeological map of Iraq, scale 1: 1000 000, 2013. *Iraqi Bulletin of Geology and Mining*, 11(1): 17-26.

Al-Jiburi, H. K., Al-Basrawi, N. H., Sissakian, V. K., Al-Ansari, N., Knutsson, S., Jasim, N. A., Sissakian, V. K., Shihab, A. T., Al-Ansari, N., Knutsson, S., Halwagy, R., Halwagy, M., Zaini, M. T. and Abdul, M. F. 2015. Hydrogeological map of Iraq, scale 1: 1000 000, 2013. *Iraqi Bulletin of Geology and Mining*, 11(1): 17-26. [CrossRef]

Al-Sababhah, N. 2023. Topographic position index to landform classification and spatial planning, using GIS, for Wadi Araba, South West Jordan. *Environment and Ecology Research*, 11(1): 79-101. [CrossRef]

Amine, A., El Amrani El Hassani, I.- E., Remmal, T., El Kamel, F., Van Wyk De Vries, B. and Boivin, P. 2019. Geomorphological classification and landforms inventory of the Middle-Atlas Volcanic Province (Morocco): Scientific value and educational potential. *Quaestiones Geographicae*, 38(1): 107-129. [CrossRef]

Burnelli, M., Melelli, L. and Alvioli, M. 2023. Land surface diversity: A geomorphodiversity index of Italy. *Earth Surface Processes and Landforms*, 48(15): 3025-3040. [CrossRef]

Carrión-Mero, P., Dueñas-Tovar, J., Jaya-Montalvo, M., Berrezueta, E. and Jiménez-Orellana, N. 2022. Geodiversity assessment to regional scale: Ecuador as a case study. *Environmental Science and Policy*, 136: 167-186. [CrossRef]

Chen, T. Y. K. and Capart, H. 2022. Computational morphology of debris and alluvial fans on irregular terrain using the visibility polygon. *Computers and Geosciences*, 169: 105228. [CrossRef]

Coulthard, T. J. 2005. Effects of vegetation on braided stream pattern and dynamics. *Water Resources Research*, 41(4): 1-9. [CrossRef]

de Amorim, L. de O., Robaina, L. E. de S. and Trentin, R. 2021. Automated analysis of landforms of the Paraguaçu River Basin / Bahia. *Revista Brasileira de Geomorfologia*, 22(3): 641-655. [CrossRef]

Flor-Blanco, G., Bruschi, V., Adrados, L., Domínguez-Cuesta, M. J., Gracia-Prieto, F. J., Llana-Fúnez, S. and Flor, G. 2022. Geomorphological evolution of the calcareous coastal cliffs in North Iberia (Asturias and Cantabria regions). *Estuarine, Coastal and Shelf Science*, 273: 107913. [CrossRef]

Ghosh, A. and Bera, B. 2023. Landform classification and geomorphological mapping of the Chota Nagpur Plateau, India. *Quaternary Science Advances*, 10: 100082. [CrossRef]

Gran, K. and Paola, C. 2001. Riparian vegetation controls on braided stream dynamics. *Water Resources Research*, 37(12): 3275-3283. [CrossRef]

Guitet, S., Cornu, J. F., Brunaux, O., Betbeder, J., Carozza, J. M. and Richard-Hansen, C. 2013. Landform and landscape mapping, French Guiana (South America). *Journal of Maps*, 9(3): 325-335. [CrossRef]

Hashemi, F., Derakhshani, R., Bafti, S. S. and Raoof, A. 2018. Morphometric dataset of the alluvial fans at the southern part of Nayband fault, Iran. *Data in Brief*, 21: 1756-1763. [CrossRef]

Kothyari, G. C., Kandregula, R. S., Chauhan, G., Desai, B. G., Taloor, A. K., Pathak, V., Swamy, K. V., Mishra, S. and Thakkar, M. G. 2021. Quaternary landform development in the central segment of tectonically active Kachchh Mainland Fault zone, Western India. *Quaternary Science Advances*, 3: 100018. [CrossRef]

Langbein, W. B. and Schumm, S. A. 1958. Yield of sediment in relation to mean annual precipitation. *Eos, Transactions American Geophysical Union*, 39(6): 1076-1084. [CrossRef]

Lee, J., Yoo, S., Kim, C. and Sohn, H. G. 2023. Automatic levee surface extraction from mobile LiDAR data using directional equalization and projection clustering. *International Journal of Applied Earth Observation and Geoinformation*, 116: 103143. [CrossRef]

Lin, S., Xie, J., Deng, J., Qi, M. and Chen, N. 2022. Landform classification based on landform geospatial structure–a case study on Loess Plateau of China. *International Journal of Digital Earth*, 15(1): 1125-1148. [CrossRef]

Ma'ala, K. A. 2009. Geomorphology of Iraqi Southern Desert. *Iraqi Bulletin of Geology and Mining*, *Special Issue, 2009: Geology of Iraqi Southern Desert*: 77-91.

Maaroof, B. F. 2022a. Geomorphological Assessment Using Geoinformatics Applications of the Sloping System of Al-Ashaali Drainage Basin at Iraqi Southern Desert. *Iraqi National Journal of Earth Science*, 22(1): 38-54. [CrossRef]

Maaroof, B. F. 2022b. Geomorphometric assessment of the river drainage network at Al-Shakak basin(Iraq). *Journal of the Geographical Institute Jovan Cvijic SASA*, 72(1): 1-13. [CrossRef]

Maaroof, B. F. 2024. Quantitative analysis using geospatial modeling of Al-Rahimawi watershed's shape properties in the Iraqi southern desert. *Bulletin of the Iraq Natural History Museum*, 18(2): 277-295. [CrossRef]

Maaroof, B. F. 2025. Fluvial landforms classification using geospatial modeling of Al-Jazeera Eastern Region at Misan Governorate, Iraq. *Iraqi National Journal of Earth Science*, 25(2), 199-218. [CrossRef]

Maaroof, B. F. and Kareem, H. H. 2020. Water erosion of the slopes of Tayyar drainage basin in the desert of Muthanna in Southern Iraq. *Indian Journal of Ecology*, 47(3): 638-644. [Click here]

Maaroof, B. F. and Kareem, H. H. 2022. Geomorphometric analysis of Al -Teeb River Meanders between Al-Sharhani Basin and Al-Sanaf Marsh, Eastern of Misan Governorate, Iraq. *Misan Journal of Academic Studies*, 42(1): 441-455. [CrossRef]

Maaroof, B. F. and Kareem, H. H. 2023. Geomorphological analysis of chemical weathering features in Al-Band Hills Area, Eastern of Misan Governorate, Iraq. *Iraqi National Journal of Earth Science*, 23(1): 67-84. [CrossRef]

Maaroof, B. F., Al-Abdan, R. H. and Kareem, H. H. 2021. Geographical assessment of natural resources at Abu-Hadair drainage basin in Al-Salman Desert. *Indian Journal of Ecology*, 48(3): 797-802. [Click here]

Maaroof, B., Omran, M., Al-Qaim, F., Salman, J., Hussain, B., Abdellatif, M., Carnacina, I., Al-Hasani, B., Jawad, M. and Hussein, W. 2023. Environmental assessment of Al-Hillah River pollution at Babil Governorate (Iraq). *Journal of the Geographical Institute Jovan Cvijic, SASA*, 73(1): 1-16. [CrossRef]

Mandal, R. and Chakrabarty, P. 2021. Badlands of Gangani in West Bengal, India: an assessment on account of geotourism development. *International Journal of Geoheritage and Parks*, 9(2): 147-156. [CrossRef]

Manosso, F. C., Zwoliński, Z., Najwer, A., Basso, B. T., Santos, D. S. and Pagliarini, M. V. 2021. Spatial pattern of geodiversity assessment in the Marrecas River drainage basin, Paraná, Brazil. *Ecological Indicators*, 126: 107703. [CrossRef]

Martins, F. M. G., Fernandez, H. M., Isidoro, J. M. G. P., Jordán, A. and Zavala, L. 2016. Classification of landforms in Southern Portugal (Ria Formosa Basin). *Journal of Maps*, 12(3): 422-430. [CrossRef]

Mirzadeh, S. M. J., Jin, S. and Amani, M. 2023. Spatial-temporal changes of Abarkuh Playa Landform from sentinel-1 time series data. *Remote Sensing*, 15(11): 2774. [CrossRef]

Mohamed, M. A. 2020. Classification of landforms for digital soil mapping in urban areas using LiDAR data derived terrain attributes: A case study from Berlin, Germany. *Land*, 9(9): 319. [CrossRef]

Mokarram, M., Roshan, G. and Negahban, S. 2015. Landform classification using topography position index (case study: salt dome of Korsia-Darab plain, Iran). *Modeling Earth Systems and Environment*, 1: 40. [CrossRef]

Mokarrama, M. and Hojati, M. 2018. Landform classification using a sub-pixel spatial attraction model to increase spatial resolution of digital elevation model (DEM). *Egyptian Journal of Remote Sensing and Space Science*, 21(1): 111-120. [CrossRef]

Morino, C., Coratza, P. and Soldati, M. 2022. Landslides, a key landform in the global geological heritage. *Frontiers in Earth Science*, 10: 864760. [CrossRef]

Nagata, T., Watanabe, Y., Yasuda, H. and Ito, A. 2014. Development of a meandering channel caused by the planform shape of the river bank. *Earth Surface Dynamics*, 2(1): 255-270. [CrossRef]

Njenga, K. J., Kwanza, J. K. and Gathia, P. J. 2012. Velocity distributions and meander formation of river channels. *International Journal of Applied Science and Technology*, 2(9): 28-39.

Olsen, N. R. B. 2021. 3D numerical modelling of braided channel formation. *Geomorphology*, 375: 107528. [CrossRef]

Pereira, D. I., Pereira, P., Brilha, J. and Santos, L. 2013. Geodiversity assessment of Paraná State (Brazil): An innovative approach. *Environmental Management*, 52(3): 541-552. [CrossRef]

Raslan, Y. and Salama, R. 2015. Development of Nile River islands between Old Aswan Dam and new Esna barrages. *Water Science*, 29(1): 77-92. [CrossRef]

Rong, T., Xu, S., Lu, Y., Tong, Y. and Yang, Z. 2022. Quantitative Assessment of Spatial Pattern of Geodiversity in the Tibetan Plateau. *Sustainability*, 15(1): 299. [CrossRef]

Sadek, N. 2013. Island development impacts on the Nile River morphology. *Ain Shams Engineering Journal*, 4(1): 25-41. [CrossRef]

Schumm, S. A. 1981. Evolution and response of the fluvial system, sedimntologic implications. *SEPM Journal of Sedimentary Research*, 31:19-29.

Singh, A., Naik, M. N. and Gaurav, K. 2022. Drainage congestion due to road network on the Kosi alluvial Fan, Himalayan Foreland. *International Journal of Applied Earth Observation and Geoinformation*, 112: 102892. [CrossRef]

Sissakian, V. K., Mahmoud, A. A. and Awad, A. M. 2013. Genesis and age determination of Al-Salman Depression, south Iraq. *Iraqi Bulletin of Geology and Mining*, 9(1): 1-16.

Swirad, Z. M. and Young, A. P. 2022. Spatial and temporal trends in California coastal cliff retreat. *Geomorphology*, 412: 108318. [CrossRef]

Tebakari, T. and Kita, R. 2015. Estimating permeability using the parameter estimation method in a High-permeability Area of the Kurobe River Alluvial Fan, Japan. *Procedia Environmental Sciences*, 25: 235-242. [CrossRef]

Teofilo, G., Gioia, D. and Spalluto, L. 2019. Integrated geomorphological and geospatial analysis for mapping fluvial landforms in Murge basse karst of Apulia (Southern Italy). *Geosciences*, 9(10): 418. [CrossRef]

Wang, Z. F., Ding, J. Y. and Yang, G. S. 2012. Risk analysis of slope instability of levees under river sand mining conditions. *Water Science and Engineering*, 5(3): 340-349. [CrossRef]

Wheaton, J. M., Fryirs, K. A., Brierley, G., Bangen, S. G., Bouwes, N. and O'Brien, G. 2015. Geomorphic mapping and taxonomy of fluvial landforms. *Geomorphology*, 248: 273-295. [CrossRef]

Xia, J., Cheng, Y., Zhou, M., Yu, X., Xu, X., Blanckaert, K. and Wang, Z. 2025. Relation between bank erosion and bed incision in the braided reach of the lower Yellow River undergoing channel degradation. *International Journal of Sediment Research*. [CrossRef]

Yang, J., Xu, J., Lv, Y., Zhou, C., Zhu, Y. and Cheng, W. 2023. Deep learning-based automated terrain classification using high-resolution DEM data. *International Journal of Applied Earth Observation and Geoinformation*, 118: 103249. [CrossRef]

Zabaleta, A., Alvarez, I., Aranburu, A., Izagirre, E., Uriarte, J. A., Morales, T. and Antiguedad, I. 2020. Landforms of the lower Hushe Valley (Central Karakoram, Pakistan). *Journal of Maps*, 16(2): 724-735. [CrossRef]

Raslan, Y. and Salama, R. 2015. Development of Nile River islands between Old Aswan Dam and new Esna barrages. *Water Science*, 29(1): 77-92. [CrossRef]

Zhou, A., Chen, Y., Wilson, J. P., Chen, G., Min, W. and Xu, R. 2023. A multi-terrain feature-based deep convolutional neural network for constructing super-resolution DEMs. *International Journal of Applied Earth Observation and Geoinformation*, 120: 103338. [CrossRef]

Bull. Iraq nat. Hist. Mus.
(2025) 18 (3): 739-763.

تصنيف الأشكال الأرضية النهرية بإستخدام النمذجة الجيومكانية لمستجمع مياه الأشعلي في صحراء العراق الجنوبية

بشار فؤاد معروف*، هاشم حنين كريم**، جعفر حسين الزبيدي***،
ريان غازي ذنون****، منال شاكر الكبيسي*****، بان الحسني******،
موده عبد العاطف****** و آياكوبو كارناسينا******

*مركز بابل للدراسات الحضارية والتاريخية، جامعة بابل، بابل، العراق.
** قسم العلوم العامة، كلية التربية الاساسية، جامعة ميسان، ميسان، العراق.
*** قسم الجيولوجيا التطبيقية، كلية العلوم، جامعة بابل، بابل ، العراق.
****مركز التحسس النائي، جامعة الموصل، الموصل، العراق.
*****قسم علوم الارض، كلية العلوم، جامعة بغداد، بغداد، العراق.
******قسم الهندسة المدنية وبيئة الأبنية، كلية التكنولوجيا الهندسية، جامعة ليفربول جون مورس، ليفربول، المملكة المتحدة.

الاستلام: 2025/2/13، المراجعة: 2025/5/27، القبول: 2025/5/29، النشر: 2025/6/20

الخلاصة

تناولت هذه الدراسة حوض تصريف الأشعلي، وهو أحد مستجمعات المياه في صحراء العراق الجنوبية، ويشكل نظاماً هيدروجيومورفولوجيًا ضمن منطقة الوديان السفلى حسب التصنيف الجيومورفولوجي للعراق. استخدمت الدراسة تقنية البكسل الثانوي لتحسين الدقة المكانية ودقة نماذج الارتفاعات الرقمية المستخدمة لتصنيف أشكال الأرض. ودمجت خرائط أشكال الأرض المشتقة من نموذج الارتفاع الرقمي SRTM مع الخرائط الطبوغرافية لفهم نشأة الاشكال الارضية في منطقة الدراسة. تم تطوير نماذج محاكاة جيومكانية لإنشاء خرائط الاشكال الارضية. و جرى تحليل البيانات باستخدام برنامج ArcGIS، والذي تضمن أدوات تلوين الخرائط وخرائط طبوغرافية وخرائط جيولوجية وهيدرولوجية. تهدف الدراسة إلى تعزيز تفسير وتحليل جيومورفولوجيا خصائص أشكال الأرض في حوض التصريف النهري. وفق نظام التصنيف الجيومورفولوجي لمعهد علوم الأرض الهولندي (ITC) صُنِفتْ أشكال الأرض في منطقة الدراسة.

أشارت النتائج إلى أن الوديان في منطقة الدراسة هي معالم أرضية تكونت خلال الزمن الرباعي وأهميتها تأتي من موقعها الحالي في المناطق القاحلة. تتعرض السهول في منطقة الدراسة للتآكل النهري وترتبط بأحواض التصريف الاخرى في منطقتها الغربية والجنوبية الغربية. وتتميز سهول التويثة بـ"مرفق الأسر" و"فجوات الرياح" بسبب التدفق المتسارع لنهر واحد مشترك. وتتأثر السهول التحاتية بعوامل التآكل، بما في ذلك ترسب الأنهار والسهول الفيضية وجزر الأنهار والجداول المضفرة. وتتطور المراوح الرسوبية في المناطق ذات المنحدرات الشديدة والأراضي المنخفضة، بينما تنشأ السهول الفيضية من الرواسب التي تحملها الوديان والجداول من المرتفعات الشديدة. وتخضع الجداول المضفرة لدورات متعددة من الترسيب والتآكل، وتتكون معظم النباتات في المنطقة من أنواع رائدة.